Efficacy of BET bromodomain inhibition in Kras-mutant non-small cell lung cancer

Takeshi Shimamura[1,*], **Zhao Chen**[2,4,5,7], **Margaret Soucheray**[1], **Julian Carretero**[8], **Eiki Kikuchi**[2,4,5,7], **Jeremy H. Tchaicha**[2,4,5,7], **Yandi Gao**[1], **Katherine A. Cheng**[2,4,5], **Travis J. Cohoon**[2,4,5], **Jun Qi**[2], **Esra Akbay**[2,4,5,7], **Alec C. Kimmelman**[3], **Andrew L. Kung**[9], **James E. Bradner**[2,10,*], and **Kwok-Kin Wong**[2,4,5,6,7,*]

[1]Department of Molecular Pharmacology and Therapeutics, Oncology Research Institute, Loyola University Chicago, Stritch School of Medicine, Maywood, Illinois, 60153, USA

[2]Department of Medical Oncology, Dana-Farber Cancer Institute, 450 Brookline Avenue, Boston, Massachusetts, 02215, USA

[3]Department of Radiation Oncology, Dana-Farber Cancer Institute, 450 Brookline Avenue, Boston, Massachusetts, 02215, USA

[4]Belfer Institute for Applied Cancer Science, Dana-Farber Cancer Institute, 450 Brookline Avenue, Boston, Massachusetts, 02215, USA

[5]Ludwig Center at Dana-Farber/Harvard Cancer Center, Dana-Farber Cancer Institute, 450 Brookline Avenue, Boston, Massachusetts, 02215, USA

[6]Lowe Center for Thoracic Oncology, Dana-Farber Cancer Institute, 450 Brookline Avenue, Boston, Massachusetts, 02215, USA

[7]Department of Medicine, Brigham and Women's Hospital, Harvard Medical School, 75 Francis Street, Boston, Massachusetts, 02115, USA

[8]Departament de Fisiologia - Facultat de Farmàcia - Universitat de València, Avda. Vicent Andrés Estellés, s/n - 46100, Burjassot, Valencia, Spain

[9]Department of Pediatrics, Columbia University Medical Center, New York, NY 10032, USA

*Corresponding authors: Kwok-Kin Wong, M.D., Ph.D., Department of Medical Oncology, Dana-Farber Cancer Institute, 450 Brookline Ave., HIM243, Boston MA, 02215, Phone: 617-632-6084; Fax: 617-632-7839; kwong1@partners.org. James E. Bradner, M.D., Ph.D., Department of Medical Oncology, Dana-Farber Cancer Institute, 450 Brookline Ave., Dana510D, Boston MA, 02215, Phone: 617-632-6629; Fax: 617-582-7370; james_bradner@dfci.harvard.edu. Takeshi Shimamura, Ph.D., Department of Molecular Pharmacology and Therapeutics, Oncology Research Institute, Loyola University Chicago Stritch School of Medicine, 2160 S 1st Avenue, Cardinal Bernardin Cancer Center 205, Maywood IL, 60153, Phone: 708-327-3250, Fax: 708-327-3238, tashimamura@lumc.edu.

[10]Department of Medicine, Harvard Medical School, 25 Shattuck Street, Boston, MA 02115, USA

Abstract

Purpose—Amplification of *MYC* is one of the most common genetic alterations in lung cancer, contributing to a myriad of phenotypes associated with growth, invasion and drug resistance. Murine genetics has established both the centrality of somatic alterations of *Kras* in lung cancer, as well as the dependency of mutant *Kras* tumors on MYC function. Unfortunately, drug-like small-molecule inhibitors of KRAS and MYC have yet to be realized. The recent discovery, in hematologic malignancies, that BET bromodomain inhibition impairs *MYC* expression and MYC transcriptional function established the rationale of targeting *KRAS*-driven NSCLC with BET inhibition.

Experimental Design—We performed functional assays to evaluate the effects of JQ1 in genetically defined NSCLC cells lines harboring *KRAS* and/or *LKB1* mutations. Furthermore, we evaluated JQ1 in transgenic mouse lung cancer models expressing mutant *kras* or concurrent mutant *kras* and *lkb1*. Effects of bromodomain inhibition on transcriptional pathways were explored and validated by expression analysis.

Results—While JQ1 is broadly active in NSCLC cells, activity of JQ1 in mutant KRAS NSCLC is abrogated by concurrent alteration or genetic knock-down of *LKB1.* In sensitive NSCLC models, JQ1 treatment results in the coordinate downregulation of the *MYC*-dependent transcriptional program. We found that JQ1 treatment produces significant tumor regression in mutant *kras* mice. As predicted, tumors from mutant *kras* and *lkb1* mice did not respond to JQ1.

Conclusion—Bromodomain inhibition comprises a promising therapeutic strategy for *KRAS* mutant NSCLC with wild-type LKB1, via inhibition of MYC function. Clinical studies of BET bromodomain inhibitors in aggressive NSCLC will be actively pursued.

Keywords

INTRODUCTION

Approximately 15 – 30% of human non-small cell lung cancer (NSCLC) patients harbor an oncogenic *KRAS* mutation associated with resistance to conventional treatment regimens (1). Oncogenic activation of *kras* in the murine lung compartment produces adenocarcinoma, and several human lung cancer cell lines harboring mutant *KRAS* are dependent on KRAS activity for survival (2–4); therefore, oncogenic mutant KRAS is a highly attractive therapeutic target in NSCLC. However, targeting mutant KRAS with small molecule inhibitors has not proven successful (1).

KRAS is a strong activator of mitogen-activated protein kinase (MAPK) and phosphatydilinositol-3-kinase (PI3K) pathways, which together confer oncogene addiction (5). In a murine lung adenocarcinoma model driven by mutant *Kras*, the concurrent inhibition of MAPK and PI3K pathways demonstrates significant tumor regression (6). Based on these preclinical data, this strategy has translated to phase I clinical trials for NSCLC patients with *KRAS* mutation. Although exact mechanisms of cell death remain elusive, several reports suggest that the inhibition of MAPK and PI3K pathways converges at the level of transcription factor MYC (7). The inhibition of KRAS-dependent MAPK and PI3K pathways results in the dephosphorylation of MYC at Serine-62 and phosphorylation at Threonine-58 (7, 8). These events contribute to rapid degradation of MYC in a proteasome-dependent manner. Several lines of evidence support a critical function for MYC in enforcing the transcriptional growth pathway downstream of *KRAS* (9). Notably,

research by Gerard Evan and colleagues has established the dependence of *KRAS*-mutated NSCLC on MYC by pharmacologic induction of a dominant-negative genetic construct, called OmoMyc (10, 11). These observations establish a pressing rationale to test therapies targeting the Myc transcriptional signaling network in *KRAS* mutant NSCLC models *in vitro* and *in vivo*.

MYC is a master regulatory transcription factor governing cellular growth, and deregulation of *MYC* in cancer contributes to proliferation, metabolic adaptation, tumorigenesis and resistance to apoptosis. Indeed, amplification of *MYC* is one of the most common genetic alterations in cancer genomes (12). MYC is a basic helix-loop-helix leucine zipper transcriptional activator and amplifier (13), which localizes to E-box binding sites at promoter and enhancer regulatory regions, as a heterodimer with Max. To date, efforts to create drug-like, direct-acting inhibitors of MYC have not been successful. This perhaps is due to the difficulty of targeting the extended protein-protein interface defined by the heterodimer and the absence of a defined ligand-binding domain (14). We have therefore undertaken an effort to impede MYC-dependent transcriptional signaling by optimizing and characterizing inhibitors of putative MYC co-activator proteins. Recently, we reported MYC-specific inhibitory activity of a highly selective inhibitor of BET bromodomains, JQ1, in models of multiple myeloma and acute leukemia (15, 16). These studies demonstrated selective inhibition of growth- and metabolism-associated transcriptional pathways characteristic of MYC function, without overt effects on other key transcriptional complexes such as AP-1 and NF- B. In an index study of BET bromodomain inhibition, we observed marked efficacy of JQ1 in models of the rare and lethal, t(15;19) subset of squamous adenocarcinoma of the head, neck and lung known as NUT midline carcinoma (17, 18). Recent research from our group has identified an inhibitory effect of BET inhibition on N-MYC function as well, in translational models of neuroblastoma (19).

Based on the rationale that BET bromodomain inhibition may confer MYC-specific anti-proliferative effects downstream of KRAS signaling, we undertook a detailed study of JQ1 in NSCLC. We have recently demonstrated that genetically-engineered mouse (GEM) models provide valuable platforms to test clinically-relevant hypotheses, which can be immediately extended to the design and implementation of human clinical trials (20). To evaluate the therapeutic efficacy of JQ1 in a common, clinically relevant subset of NSCLC, we performed genetic and functional analyses to assess the impact of JQ1 treatment in mouse lung tumors.

MATERIALS AND METHODS

Cell lines and viability assays

NSCLC cell lines were obtained from the American Type Culture Collection (ATCC) and were maintained as specified. The cells lines were tested by a certified third party laboratory for authenticity (See Supplementary Methods). JQ1 was dissolved in cell culture grade dimethylsulfoxide (DMSO; Sigma). Cell viability assay was performed as described previously (21), and as detailed in Supplementary Methods.

Western blot analysis

Lysate preparation and Western blot were performed as described previously (22). Detailed methods and a list of antibodies used are available in Supplementary Methods.

Luminex Assay

Luminex-based multi-bead assays were carried out as described previously (21). Briefly, quantification of MYC and apoptosis were assayed using the Milliplex Pluripotent Stem Cell Assay and Milliplex Human Apoptosis Assay, respectively (Millipore).

shRNA constructs, lentiviral infection, and siRNA transfection

pLKO.1 short hairpin RNA (shRNA) constructs designed by the Harvard RNAi consortium and siRNA (Thermo) was used as described previously (22). shRNA sequences and procedures are provided in Supplementary Methods.

Analysis of Microarray Gene Expression Data

Gene expression profiling methods (Total RNA isolation and microarray processing) are available in Supplementary Methods.

Murine drug treatment studies

Genetically engineered mice harboring a conditional activating mutation (G12D) at the endogenous *Kras* locus, conditional *Lkb1* knockout, and conditional *p53* knockout have been described previously (21, 23). All animal treatment studies were reviewed and approved by the IACUC at the Dana-Farber Cancer Institute. *Kras* and *Kras/Lkb1* mice were treated with 5×10^6 p.f.u. adeno-Cre (University of Iowa viral vector core) intranasally as previously described (20, 21, 23), and subjected to magnetic resonance imaging (MRI) to document tumor burden. After initial imaging, animals were subjected to treatment with JQ1 formulated in 10%DMSO, 90% 10%-Hyroxypropyl Beta Cyclodextrin and given IP route at 50 mg/kg or vehicle daily. Primary lung tumors were macrodissected and formalin fixed or frozen in liquid nitrogen and stored at −80°C until use.

Imaging with tumor volume measurement and immunohistochemistry

MRI measurements were performed as previously described (20), to determine the reduction in tumor volume after the indicated time of treatment. Using the RARE sequence scans, tumor volume measurements were generated using in-house custom software. 3D Slicer was used to reconstruct MRI volumetric measurements as reported previously (20). All murine FDG-PET/CT studies were performed with a preclinical small animal PET/CT system (Siemens Inveon) after injection with 14MBq of 18F-FDG as previously reported (20). Immunohistochemistry was performed as described previously (20). Details and a list of antibodies used is available in the Supplementary Methods.

Statistical analysis

Unless otherwise stated, comparisons of statistical significance were performed using the Student's *t*-test. A p-value < 0.05 was considered statistically significant.

RESULTS

JQ1 is active in NSCLC cells of different genotypes, but concomitant alteration of *KRAS* and *LKB1* confers resistance

To evaluate the efficacy of BET bromodomain inhibition in NSCLC, human cell lines bearing mutations in *KRAS* were first screened for sensitivity to the prototype BET inhibitor, JQ1. Unlike hematologic malignancies, where uniform activity of JQ1 is observed, 24 NSCLC cell lines displayed clear dose-dependent sensitivity or resistance to bromodomain inhibition (Supplementary Fig. 1A and 1B). Anti-proliferative activity of BET inhibition was observed in all genetically-defined subtypes of NSCLC, but closer inspection

of common genetic alterations revealed reduced efficacy when *LKB1* and *KRAS* were both altered (Fig. 1A). In total, 8 out of 24 cells lines tested harbor *KRAS* mutation and 3 of 4 cell lines with concurrent *KRAS* and *LKB1* mutation are found to be resistant to JQ1. In contrast, the 4 out of 4 *KRAS* mutated cell lines without *LKB1* mutation responded to JQ1 treatment. Among the 24 cell lines tested, no predictive correlation was observed based on KRAS or EGFR mutational status (Supplementary Fig. 1C). Growth rates of cells under JQ1 treatment were compared to the expression levels of bromodomain and extra-terminal (BET) family proteins and genotype data extracted from the Cancer Cell Line Encyclopedia (CCLE) dataset (Fig. 1B). No significant correlation was found between growth inhibition by JQ1 and the expression level of BET genes (*BRD2*, *BRD3*, *BRD4* and *BRDT*).

JQ1-induced apoptosis in KRAS mutant NSCLC cells is abrogated with concurrent LKB1 mutation

We next investigated whether BET bromodomain inhibition in mutant *KRAS* NSCLC promotes apoptosis. We employed Luminex-based apoptosis assays measuring activated (cleaved) caspase 3 and cleaved-PARP following 48 hours of JQ1 or DMSO (vehicle) treatment in NCI-H441 (mutant *KRAS*) and A549 (*KRAS/LKB1* mutant) cells. These two cell lines showed markedly different apoptotic responses (Fig. 1C). Robust and dose-dependent increases in activated Caspase-3 and cleaved PARP were evident in H441 cells. In contrast, induction of apoptosis was subtle in A549 cells. Similarly, JQ1 treatment induced apoptosis in SK-LU-1 cells harboring mutant *KRAS* but not in NCI-H460 cells with *KRAS/LKB1* mutation (Supplementary Fig. 1D). Cell viability assays confirmed the differences in apoptotic response to JQ1 treatment (Supplementary Fig. 1E).

MYC expression in *KRAS* positive NSCLC is BRD4 dependent but only in the absence of *LKB1* mutation

To investigate the molecular determinants of differences observed between *KRAS* mutant and *KRAS/LKB1* mutant cells, we treated NCI-H441 (KRAS^{G12V}), NCI-H1734 (KRAS^{G13C}), A549 (KRAS^{G12S}/LKB1^{mut}), and NCI-H460 (KRAS^{Q61K}/LKB1^{mut}) cells with JQ1 for 48 hours (Fig. 2). Among these cell lines, NCI-H441 and A549 human cell lines have been functionally validated as strongly dependent on KRAS-mediated signaling (4, 24). Proliferation assays demonstrated that H441 cells were sensitive to JQ1 with an IC$_{50}$ of 0.06 μM while A549 cells were resistant to JQ1 with an IC$_{50}$ higher than 10 μM (Supplementary Fig. 1A). Similarly, H460 cells harboring LKB1-mutant are resistant to JQ1 with IC$_{50}$ around 10 μM (Supplementary Fig. 1E).

We have demonstrated in highly sensitive hematologic malignancies that the observed, potent antiproliferative effect of BET bromodomain inhibition is variably associated with rapid downregulation of *MYC* (15). Therefore, we investigated how JQ1 treatment affects *MYC* expression across a panel of NSCLC cells. All cell lines tested expressed *MYC* and *BRD4*, with some variability in expression levels. As a technical note, we detected multiple electrophoretic bands by immunoblot with an anti-MYC antibody. To identify the correct MYC protein, we repeated the immunoblot using lysates harvested from A549, H441, and SK-LU-1 cells transduced with lentivirus coding for non-target and *MYC* (Supplementary Fig. 2A). As expected, a 57kDa reacting band was the only band depleted by *MYC* specific shRNA. Following 48 hours of JQ1 exposure, the 57kDa MYC was depleted in JQ1-sensitive H441 and H1734 cells. No effect was observed on MYC expression in resistant A549 and H460 cells (Fig. 2A). To quantify the expression of the 57kDa MYC protein in H441 and A549 cells upon JQ1 treatment, a sensitive Luminex-based assay was performed. The assay independently confirmed depletion of MYC in H441 cells in a dose-dependent manner, in contrast to resistant A549 cells (Fig. 2B). Time-dependent inhibition of MYC

expression in sensitive H441 cells was demonstrated by immunoblot. H441 cells exposed to 250 nM of JQ1 begin to deplete MYC in 8 hours (Supplementary Fig. 2B).

Interestingly, exposure to JQ1 also promoted accumulation of BRD4 in cellular lysates within 2 hours (Supplementary Fig. 2B). As BRD4 and MYC primarily localize to the nucleus, we examined the compartment-specific enrichment of BRD4 and MYC in H441 cells upon JQ1 treatment (Fig. 2C). In H441 cells, JQ1 treatment promoted increased appearance of BRD4 in the cytosol and depletion of MYC in the nucleus, illustrating the effect of JQ1 on BET bromodomain displacement from chromatin and corroborating the marked effect on *MYC* expression.

BRD4 knockdown in H441 cells recapitulates effects of JQ1 in H441 cells

To understand the mechanism of *MYC* transcriptional inhibition, we assessed function of BET bromodomain proteins in enforcing *MYC* expression. H441 and A549 cells were transduced with two lentiviral shRNA vectors designed to target BRD4 or a control (non-target) shRNA, followed by puromycin selection. Within 96 hours post lentiviral transduction, BRD4 was significantly (>80%) depleted (Fig. 2D). RNA interference of BRD4 expression resulted in marked reduction in MYC by immunoblot in JQ1-sensitive H441 cells but not in JQ1-resistant A549 cells. In addition, the cell viability of H441 was significantly reduced by BRD4 shRNA at 7 days post-infection (p < 0.01), whereas only a minimal effect on A549 cell viability was observed (less than 50% reduction; Fig. 2E).

MYC transcriptional programs are arrested in JQ1-sensitive mutant *KRAS* positive NSCLC cells

We have observed in highly sensitive hematologic malignancies that rapid downregulation of MYC expression is accompanied by suppression of the *MYC*-dependent transcriptional growth program (15). To investigate the effect of BET inhibition on NSCLC transcriptional pathways, we performed genome-wide transcriptional profiling of NSCLC cells treated with JQ1 or vehicle control. Unsupervised hierarchical clustering of replicate samples readily identified JQ1 versus vehicle treated samples. Effects on *MYC*-specific transcription were investigated using reported, functionally validated gene signatures correlating with deregulated *MYC* (15, 16, 25, 26). All MYC signatures were strongly correlated with downregulation of gene expression by JQ1 in NCI-H441 cells (Fig. 3A). To ascertain whether the H441 cells are MYC dependent, we depleted MYC using lentiviral shRNA (Fig. 3B). Five days post infection, the viability of H441 cells following *MYC* knockdown was significantly reduced compared to cells infected with virus expressing control shRNA (p < 0.01). In a sharp contrast, MYC depletion in JQ1-resistant A549 cells by lentiviral shRNA did not affect viability.

LKB1 mutational status determines sensitivity to JQ1 in mutant *KRAS* positive NSCLC cells

We have demonstrated that the efficacy of JQ1 and dependency on the BRD4-MYC axis is determined by the mutational status of LKB1 in mutant KRAS NSCLC cell lines. To confirm and extend this finding, we assessed whether loss of LKB1 alone impacts the cellular response to JQ1 treatment, using isogenic paired cell lines (NCI-H358 and NCI-H441) expressing shRNA to LKB1 (LKB1), a non-targeting shRNA (NT). Immunoblot analysis of cells treated with JQ1 (500 nM for 48 hours) or vehicle control demonstrated that LKB1 knock-down impairs the robust inhibition of MYC expression observed with JQ1 (Fig. 4A). We then explored the effect of forced expression of LKB1 in a *LKB1* mutated, JQ1 resistant cell line. In contrast to vector-transduced, control A549 cells, LKB1 overexpressing A549 cells exhibited downregulation of MYC by JQ1 (Fig. 4A). After 48 hours of BET inhibition, LKB1 transduced A549 cells now exhibited induction of markers

of late apoptosis, cleaved PARP and cleaved caspase 3 (Fig. 4B). The A549 cells transduced with vector control failed to undergo programmed cell death, compared to untreated controls (Fig. 4B).

Efficacy of BET bromodomain inhibition in GEM models of KRAS mutated NSCLC

Having demonstrated that a subset of NSCLC cells harboring mutant KRAS are dependent on the BRD4-MYC transcriptional axis, we next explored the therapeutic relevance of BET bromodomain inhibition using genetically engineered mice (GEM) with either mutant *kras* or mutant *kras/lkb1*. Activation of mutant *kras* (G12D) and inactivation of *lkb1* in the lung epithelium was initiated using nasal instillation of adenovirus encoding the CRE recombinase. Mice with established tumors, defined by evident and significant tumor burden by magnetic resonance imaging (MRI), were treated with 50 mg/kg JQ1 or vehicle control by intraperitoneal injection. Response to treatment was monitored by serial MRI imaging (Fig. 5A). Tumor volume in response to therapy was determined by previously validated, quantitative methods (20). Among mice with *kras* mutant tumors, single agent JQ1 provoked a partial response in 100 % of treated animals, defined by a greater than 30 % reduction in tumor volume (Fig. 5A and Fig. 5B). Mice bearing *kras* mutant tumors responded significantly better than mice with mutant *kras* tumors with concurrent *lkb1* loss (Fig. 5A and Fig. 5B; Fisher's exact test, p = 0.015).

To further explore early tumor metabolic changes following JQ1 therapy, FDG-PET/CT was performed on mutant *kras* mice at pre- and post- three days of JQ1 treatment. Treatment with JQ1 resulted in significant changes in tumor hyper-metabolism in mice with mutant *kras* tumors (Fig. 5C). Together, these results demonstrate that changes in tumor metabolism measured by FDG-PET/CT are in agreement with the volumetric analyses of tumor burden using MRI (Fig. 5A and 5C), and that both reveal tumor regressions in mutant *kras* tumors with single-agent BET bromodomain inhibition.

Histologic confirmation of radiographic responses to JQ1 treatment in mutant *kras* mice

To confirm the radiographic responses in *kras* mice, we performed a detailed immunohistochemical examination of tumor tissue isolated from treated animals. For these pharmacodynamic studies, mice were treated with three daily doses of vehicle or JQ1 prior to sacrifice and harvest of tumors for immunohistochemical analysis. In *kras* mice, JQ1 treatment resulted in increased staining for brd4 decreased staining for myc (Fig. 5D, left). In contrast, JQ1 treatment failed to deplete myc in mutant *kras/lkb1* mice (Fig. 5D, right) while brd4 staining increased upon JQ1 treatment, consistent with our human cell line data (Fig. 2A). To confirm *myc* depletion in mutant *Kras* mice, total RNA was isolated from both JQ1 treated and vehicle treated tumor nodules and evaluated by real time PCR using probes specific to murine *myc* (Fig. 5E). Pharmacologic exposure to JQ1 significantly (p < 0.006) reduced transcription of *myc* in mutant *kras* mouse tumors.

Measurements of tumor volume confirmed that NSCLC tumors with mutant *kras* are considerably more responsive to JQ1 than tumors with combined alteration of *kras* and *lkb1*. Consistently, histopathological examination of tumors collected after 3 days of treatment revealed that BET inhibition produced a significant increase in apoptosis (p = 0.0075, Supplementary Fig. 4A) and reduction in proliferation (p < 0.05, Fig. 5F and G) in the mutant *Kras* tumors but not in *Kras/Lkb1* mutant tumors.

DISCUSSION

While direct inhibition of KRAS remains a formidable challenge in the field of cancer drug discovery, the ultimate dependency of Ras signaling on MYC affords new opportunities for

drug development within chromatin-dependent transcriptional signaling pathways. The emergence of BET bromodomain proteins as novel co-activators of *MYC* expression and function prompted consideration of this emerging class of investigational cancer agents as therapeutics for KRAS-dependent NSCLC.

Among 24 NSCLC cell lines representing the clinically apparent genotypes defining aggressive NSCLC, BET bromodomain inhibition confers a meaningful but highly variable response. Cytotoxic activity was not correlated with *KRAS* and *EGFR* mutational status; however, the increased fraction of resistant cell lines harboring both *KRAS* and *LKB1* alterations prompted further mechanistic and translational interrogation. Interestingly, we observe that the downregulation of MYC expression and function by BET bromodomain inhibition is highly influenced by LKB1 status. We speculate that altered cell signaling in the context of *LKB1* loss produces divergent enforcement of *MYC* expression.

The results with BRD4 knockdown (Fig. 2D and E) and MYC knockdown (Fig. 3B) suggest that MYC depletion following inhibition of BRD4 by JQ1 treatment is detrimental to NSCLC cells harboring mutant KRAS as evidenced by decreased cell viability and increased apoptosis. In contrast, JQ1 treatment in KRAS/LKB1 mutant cells does not promote the depletion of MYC (Fig. 2B). Similarly, the depletion of BRD4 in A549 cells did not result in the depletion of MYC (Fig. 2D), suggesting, but not proving, that the interactions between BRD4 and MYC in KRAS/LKB1 mutant cells are distinct from those in KRAS mutant cells.

Previously, we have reported that murine tumors with both *kras* and *lkb1* mutations are highly metastatic and respond poorly to simultaneous inhibition of PI3K and MAPK pathways (6, 21). This observation suggests that *LKB1* deletion impacts how mutant KRAS regulates PI3K and MAPK pathway activity. The differential activation of the PI3K and MAPK pathways by mutant KRAS in the absence of LKB1 might also promote cellular independence from *MYC* transcriptional activity, as PI3K and MAPK signaling activities have been shown to control MYC turnover (7, 9). Ongoing research in our laboratory using genome-wide chromatin immunoprecipitation will explore differential enhancer structure and function in the *MYC* gene desert.

Of note, murine NSCLC tumors harboring mutant *kras* were sensitive to BET bromodomain inhibition; however, not all human mutant *KRAS* NSCLC cell lines are sensitive to the inhibition. The discrepancy in the response to JQ1 may be due to the fact that the genetically engineered mouse model used in this study is *kras*-driven while not all human NSCLC cell lines harboring mutant KRAS are driven by mutant KRAS as reported previously (3, 4, 24, 27). The difference in cellular dependency on mutant KRAS may impact how the cells utilize myc function, ultimately influencing on how the cells respond to BET bromodomain inhibitors. Future work to investigate the impact of BET bromodomain inhibition on MYC-driven NSCLC cells with or without mutant KRAS will provide more mechanistic insights.

To confirm that mutational status of LKB1 determines the antitumoral activity of JQ1 in NSCLC harboring mutant KRAS, we generated a set of isogenic cell lines where LKB1 was restored (in mutated resistant cells) or enforced (in wild-type sensitive cells; Fig. 4). Together these studies confirmed the pronounced effect of LKB1 status on JQ1 sensitivity and JQ1-dependent MYC downregulation.

While these studies were being completed, Lockwood *et al.* reported the suppression of the oncogenic transcription factor FOSL1 by BET bromodomain inhibition, also using the JQ1 chemical probe from the Bradner laboratory (28). To confirm these observations, we treated JQ1 sensitive NCI-H441 with dose-ranging JQ1 for 48 hours (Supplementary Fig. 3A). Whole cell lysates were subjected to Western blot using MYC and FOSL1 antibodies. We

observed dose-dependent depletion of MYC and FOSL1, though MYC exhibited comparatively increased sensitivity to BET inhibition.

To explore whether FOSL1 depletion by JQ1 explains the differential responses to JQ1 in mutant KRAS NSCLC cell lines with or without LKB1, whole cell lysates from isogenic paired cell lines treated with JQ1 or DMSO were subjected to immunoblot for FOSL1 (Supplementary Fig. 3B). In the paired H441 cell lines, the depletion of FOSL1 by JQ1 treatment did not differ between LKB1 expressing and deficient cells. In the paired resistant A549 cells, basal FOSL1 expression level was higher in the LKB1 reconstituted cells, but JQ1 treatment depleted FOSL1 in both sensitive and resistant cells. These data suggest that the suppression of FOSL1 may not entirely explain the differential effect of JQ1 in LKB1 deficient and proficient NSCLC cell lines harboring KRAS mutation. *In vivo*, JQ1 treatment did not promote *fosl1* transcript depletion in murine mutant *kras* tumors (Data not shown). Further collaborative research will help to contextualize effects on these two BET-responsive master regulatory transcription factors.

Interestingly, the exposure to JQ1 promoted nuclear accumulation of BRD4 in all the NSCLC cell lines tested (Fig. 2A and 2C). The rapid increase in BRD4 staining by immunoblot (Supplementary Fig. 2B) may relate to competitive binding of JQ1 with chromatin, consistent with increased free BRD4 that could have significance for pharmacodynamic biomarker development.

Here, we provide a chemical strategy to inhibit *MYC* transcriptional signaling downstream of mutant KRAS in lung adenocarcinoma, a common and aggressive human malignancy. Single-agent efficacy of BET bromodomain inhibition in NSCLC has been demonstrated in GEM models of *Kras* mutant NSCLC. Use of multiallelic GEM models identifies a genetically-defined cohort of patients unlikely to respond, guiding patient selection. Together, these data and insights will guide immediate human clinical investigation of clinical BET inhibitors in early-stage cancer clinical trials.

Supplementary Material

Refer to Web version on PubMed Central for supplementary material.

Acknowledgments

References

1. Pylayeva-Gupta Y, Grabocka E, Bar-Sagi D. RAS oncogenes: weaving a tumorigenic web. Nat Rev Cancer. 2011; 11:761–74. [PubMed: 21993244]

2. Johnson L, Mercer K, Greenbaum D, Bronson RT, Crowley D, Tuveson DA, et al. Somatic activation of the K-ras oncogene causes early onset lung cancer in mice. Nature. 2001; 410:1111–6. [PubMed: 11323676]

3. Luo J, Emanuele MJ, Li D, Creighton CJ, Schlabach MR, Westbrook TF, et al. A genome-wide RNAi screen identifies multiple synthetic lethal interactions with the Ras oncogene. Cell. 2009; 137:835–48. [PubMed: 19490893]

4. Singh A, Greninger P, Rhodes D, Koopman L, Violette S, Bardeesy N, et al. A gene expression signature associated with "K-Ras addiction" reveals regulators of EMT and tumor cell survival. Cancer Cell. 2009; 15:489–500. [PubMed: 19477428]

5. Malumbres M, Barbacid M. RAS oncogenes: the first 30 years. Nat Rev Cancer. 2003; 3:459–65. [PubMed: 12778136]

6. Engelman JA, Chen L, Tan X, Crosby K, Guimaraes AR, Upadhyay R, et al. Effective use of PI3K and MEK inhibitors to treat mutant Kras G12D and PIK3CA H1047R murine lung cancers. Nat Med. 2008; 14:1351–6. [PubMed: 19029981]

7. Sears R, Nuckolls F, Haura E, Taya Y, Tamai K, Nevins JR. Multiple Ras-dependent phosphorylation pathways regulate Myc protein stability. Genes Dev. 2000; 14:2501–14. [PubMed: 11018017]

8. Pelengaris S, Khan M, Evan G. c-MYC: more than just a matter of life and death. Nat Rev Cancer. 2002; 2:764–76. [PubMed: 12360279]

9. Yeh E, Cunningham M, Arnold H, Chasse D, Monteith T, Ivaldi G, et al. A signalling pathway controlling c-Myc degradation that impacts oncogenic transformation of human cells. Nat Cell Biol. 2004; 6:308–18. [PubMed: 15048125]

10. Soucek L, Whitfield J, Martins CP, Finch AJ, Murphy DJ, Sodir NM, et al. Modelling Myc inhibition as a cancer therapy. Nature. 2008; 455:679–83. [PubMed: 18716624]

11. Soucek L, Whitfield JR, Sodir NM, Masso-Valles D, Serrano E, Karnezis AN, et al. Inhibition of Myc family proteins eradicates KRas-driven lung cancer in mice. Genes Dev. 2013; 27:504–13. [PubMed: 23475959]

12. Beroukhim R, Mermel CH, Porter D, Wei G, Raychaudhuri S, Donovan J, et al. The landscape of somatic copy-number alteration across human cancers. Nature. 2010; 463:899–905. [PubMed: 20164920]

13. Lin CY, Loven J, Rahl PB, Paranal RM, Burge CB, Bradner JE, et al. Transcriptional Amplification in Tumor Cells with Elevated c-Myc. Cell. 2012; 151:56–67. [PubMed: 23021215]

14. Darnell JE Jr. Transcription factors as targets for cancer therapy. Nat Rev Cancer. 2002; 2:740–9. [PubMed: 12360277]

15. Delmore JE, Issa GC, Lemieux ME, Rahl PB, Shi J, Jacobs HM, et al. BET bromodomain inhibition as a therapeutic strategy to target c-Myc. Cell. 2011; 146:904–17. [PubMed: 21889194]

16. Zuber J, Shi J, Wang E, Rappaport AR, Herrmann H, Sison EA, et al. RNAi screen identifies Brd4 as a therapeutic target in acute myeloid leukaemia. Nature. 2011; 478:524–8. [PubMed: 21814200]

17. Bauer DE, Mitchell CM, Strait KM, Lathan CS, Stelow EB, Luer SC, et al. Clinicopathologic Features and Long-term Outcomes of NUT Midline Carcinoma. Clin Cancer Res. 2012; 18:5773–9. [PubMed: 22896655]

18. Filippakopoulos P, Qi J, Picaud S, Shen Y, Smith WB, Fedorov O, et al. Selective inhibition of BET bromodomains. Nature. 2010; 468:1067–73. [PubMed: 20871596]

19. Puissant A, Frumm SM, Alexe G, Bassil CF, Qi J, Chantery YH, et al. Targeting MYCN in neuroblastoma by BET bromodomain inhibition. Cancer Discov. 2013; 3:308–23. [PubMed: 23430699]

20. Chen Z, Cheng K, Walton Z, Wang Y, Ebi H, Shimamura T, et al. A murine lung cancer co-clinical trial identifies genetic modifiers of therapeutic response. Nature. 2012; 483:613–7. [PubMed: 22425996]

21. Carretero J, Shimamura T, Rikova K, Jackson AL, Wilkerson MD, Borgman CL, et al. Integrative genomic and proteomic analyses identify targets for Lkb1-deficient metastatic lung tumors. Cancer Cell. 2010; 17:547–59. [PubMed: 20541700]

22. Shimamura T, Li D, Ji H, Haringsma HJ, Liniker E, Borgman CL, et al. Hsp90 inhibition suppresses mutant EGFR-T790M signaling and overcomes kinase inhibitor resistance. Cancer Res. 2008; 68:5827–38. [PubMed: 18632637]

23. Ji H, Ramsey MR, Hayes DN, Fan C, McNamara K, Kozlowski P, et al. LKB1 modulates lung cancer differentiation and metastasis. Nature. 2007; 448:807–10. [PubMed: 17676035]

24. Scholl C, Frohling S, Dunn IF, Schinzel AC, Barbie DA, Kim SY, et al. Synthetic lethal interaction between oncogenic KRAS dependency and STK33 suppression in human cancer cells. Cell. 2009; 137:821–34. [PubMed: 19490892]

25. Schlosser I, Holzel M, Hoffmann R, Burtscher H, Kohlhuber F, Schuhmacher M, et al. Dissection of transcriptional programmes in response to serum and c-Myc in a human B-cell line. Oncogene. 2005; 24:520–4. [PubMed: 15516975]

26. Schuhmacher M, Kohlhuber F, Holzel M, Kaiser C, Burtscher H, Jarsch M, et al. The transcriptional program of a human B cell line in response to Myc. Nucleic Acids Res. 2001; 29:397–406. [PubMed: 11139609]

27. Barbie DA, Tamayo P, Boehm JS, Kim SY, Moody SE, Dunn IF, et al. Systematic RNA interference reveals that oncogenic KRAS-driven cancers require TBK1. Nature. 2009; 462:108–12. [PubMed: 19847166]

28. Lockwood WW, Zejnullahu K, Bradner JE, Varmus H. Sensitivity of human lung adenocarcinoma cell lines to targeted inhibition of BET epigenetic signaling proteins. Proc Natl Acad Sci U S A. 2012; 109:19408–13. [PubMed: 23129625]

TRANSLATIONAL RELEVANCE

Preclinical studies have played a key role in defining NUT midline carcinoma, multiple myeloma, and acute myeloid leukemia as diseases leveraged for sensitivity to bromodomain inhibition. Here, we provide a mechanistic rationale for the clinical study of bromodomain inhibitors in non-small cell lung cancer (NSCLC). Using validated models of NSCLC *in vitro* and *in vivo*, we provide experimental evidence that the prototype BET bromodomain inhibitor, JQ1, exerts remarkable anti-tumor efficacy in a subset of NSCLC cells harboring *KRAS* mutation. Sensitivity to bromodomain inhibition is highly influenced by *LKB1* mutation status, as Kras/Lkb1 mutant tumor models are comparatively more resistant. Furthermore, the series of *in vivo* experiments using genetically engineered mouse lung cancer models described in this manuscript confirmed that single-agent bromodomain inhibition prompts *bona fide* tumor regression in mutant *Kras* mouse lung cancers. Consistent with cultured human cell lines, *Kras/Lkb1* mutant tumors were less responsive to the bromodomain inhibitor. Sensitivity both *in vitro* and *in vivo* is mediated by down-regulation of MYC, a known master regulatory transcription factor downstream of the KRAS signaling pathway. The data presented in this manuscript identifies a genetically-defined cohort of patients unlikely to respond to JQ1 treatment, guiding patient selection in early-stage cancer clinical trials.
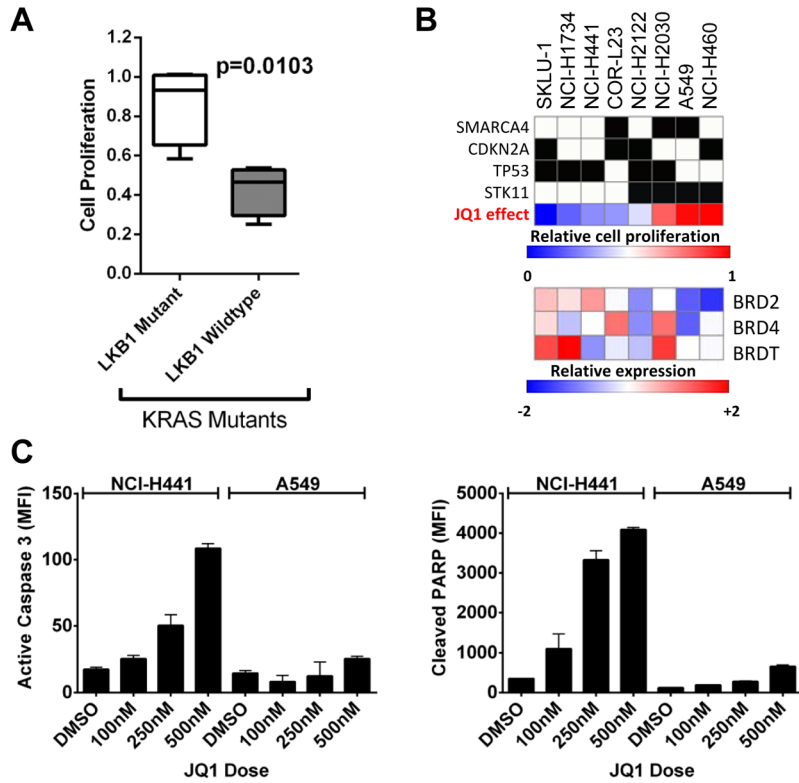
Figure 1. JQ1 treatment induces apoptosis in NSCLC cells with mutant KRAS but not KRAS/ LKB1 mutant cells

(A) NSCLC cells with KRAS/LKB1 mutations (Left, Open box) proliferate faster than NSCLC cells with KRAS mutation and wild-type LKB1 (Right, grey box) in the presence of JQ1. The proliferation rates of cells treated with 2.5 μM JQ1 were compared to that of cells in DMSO. Proliferation rates of the 24 cell lines tested are listed in Supplementary Fig. 1B. (B) Growth retardation by JQ1 treatment and genotypic characteristics of NSCLC cells harboring *KRAS* mutation. Percent growth with JQ1 in blue indicates small or no growth inhibition, while red indicates growth despite exposure to JQ1. In the heat map showing the expression level of BRD2, 4, and T, low relative expressions are represented by blue and high expression is indicated by red. (C) Exponentially growing NCI-H441 (KRAS^{mut}/ LKB1^{WT}) cells or A549 (KRAS^{mut}/LKB1^{mut}) cells were treated with DMSO or indicated doses of JQ1 for 48 hours. Cells were harvested for Luminex-based active Caspase 3 (Left) and cleaved PARP (Right) assay for the detection of apoptosis. Dose dependent induction of activated Caspase-3 and cleaved PARP is evident in H441 cells but not in A549 cells. The results are from two independent experiments run with duplicate samples. Bars, S.D.
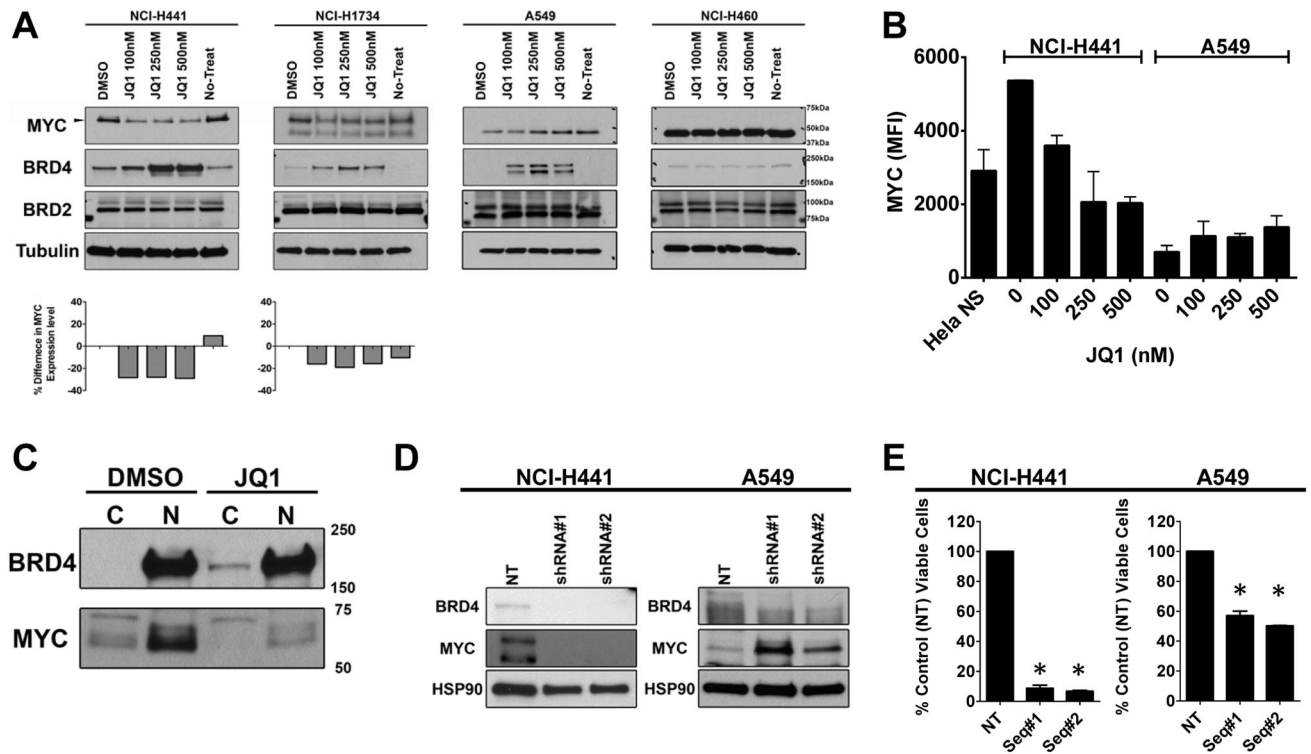
Figure 2. JQ1 promotes depletion of MYC in NSCLC cells with mutant KRAS

(A) A panel of exponentially growing NSCLC cells (NCI-H441 and NCI-H1734 cells are with KRAS^{mut}/LKB1^{WT} and A549 and NCI-H460 cells are with KRAS^{mut}/LKB1^{mut}) were treated with indicated doses of JQ1 for 48 hr and lysates were prepared for Western blotting with the indicated antibodies and demonstrate dose dependent accumulation of BRD4. Note that JQ1 induced depletion of MYC (57kDa) is evident in KRAS^{mut}/LKB1^{WT} cells. MYC (57kDa) was not detectable in KRAS^{mut}/LKB1^{mut} cells with the film exposure time. (B) NCI-H441 or A549 cells were treated with DMSO or indicated doses of JQ1 for 48 hours. Cells were harvested for a Luminex assay to quantify the MYC abundance. Units are mean fluorescent intensity (MFI) and the number is proportional to the amount of protein in the cell. The results represent an average of two independent assays run in duplicate samples. (C) Exponentially growing NCI-H441 cells (KRAS^{mut}/LKB1^{WT}) were treated with 500 nM JQ1 or vehicle for 48 hours and lysates were harvested. The cytosolic (C) and nuclear (N) fractions were prepared and the samples were subjected to Western blotting with the indicated antibodies, demonstrating the accumulation of BRD4 takes place in the cytosol and MYC depletion takes place in the nucleus. (D) A representative Western blot showing NCI-H441 or A549 cells transduced with lentiviruses encoding two shRNA sequences targeting BRD4 or a shRNA sequence control. Western blots were performed 5 days post-transduction; in each case, the control construct did not reduce expression of BRD4. In H441 cells, BRD4 knockdown promoted the decrease of MYC expression while BRD4 knockdown in A549 resulted in an increase of MYC expression. (E) Viability assays were performed 7 days after infection, and viability was normalized to cells infected with a lentivirus encoding a non-targeting shRNA. Columns represent the average of triplicate samples. The viability for H441 and A549 cells was significantly (*) reduced by BRD4 knockdown with the most profound reduction being observed in H441 cells. Results represent an average of two independent assays. Bars, SD.

A

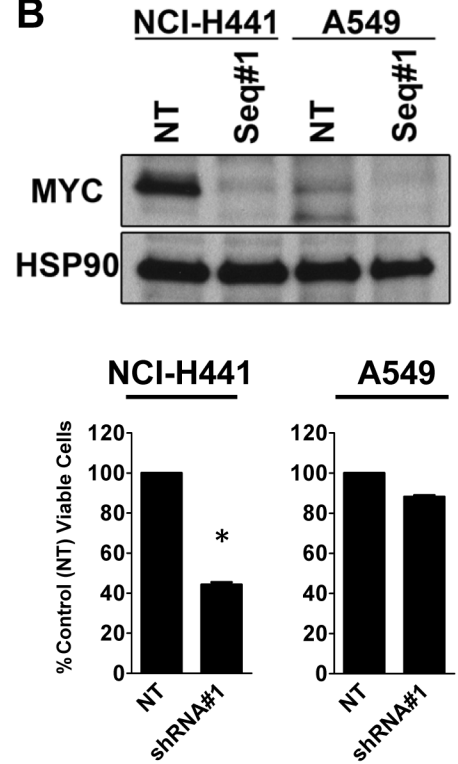| GENE SET	N	NES	FDR q-val
DELMORE_JQ1_DOWN	382	2.2	<0.0001
SCHUHMACHER_MYC_TARGETS_UP	63	1.8	0.003
MYC_ONCOGENIC_SIGNATURE	173	1.6	0.02
ZUBER_BRD4_KD_DOWN	167	1.6	0.03
MANALO_HYPOXIA_UP	91	1.5	0.03
SCHLOSSER_MYC_TARGETS_AND_SERUM_RESPONSE_UP	46	1.5	0.04
YU_MYC_TARGETS_UP	34	1.5	0.05
RIBOSOME_BIOGENESIS_AND_ASSEMBLY	14	1.4	0.05
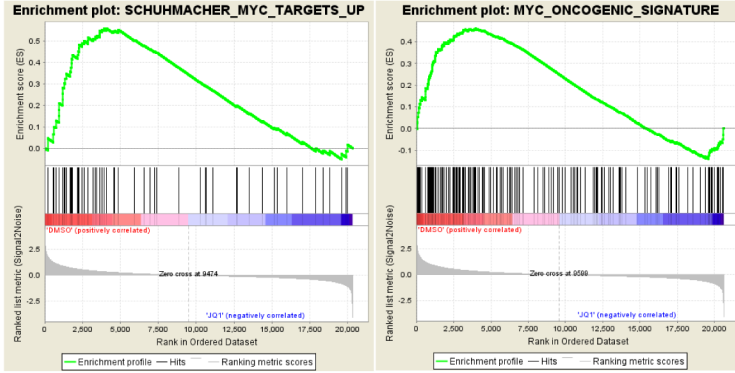
B

Figure 3. JQ1 suppresses the MYC transcriptional program and depletion of MYC phenocopies the JQ1 effect in H441 KRAS^{mut}/LKB1^{WT} NSCLC cells

(A) Table of gene sets enriched among genes downregulated by JQ1-treatment in NCI-H441 cells. N: the number of genes in gene set, NES: the normalized enrichment score, and FDR q-val: statistical significance of FDR test. *MYC* gene sets are significantly downregulated in JQ1-treated NCI-H441 cells. (B) NCI-H441 or A549 cells were transduced with lentiviruses encoding two different sequences of shRNAs targeting MYC or non-target shRNA (control). Western blots were performed 5 days post-transduction; in each case, the control construct did not reduce expression of MYC. In H441 cells, MYC knockdown promoted the significant (*, $p < 0.01$) decrease in cell viability while MYC depletion in A549 demonstrates no growth retardation. Bars, SD.
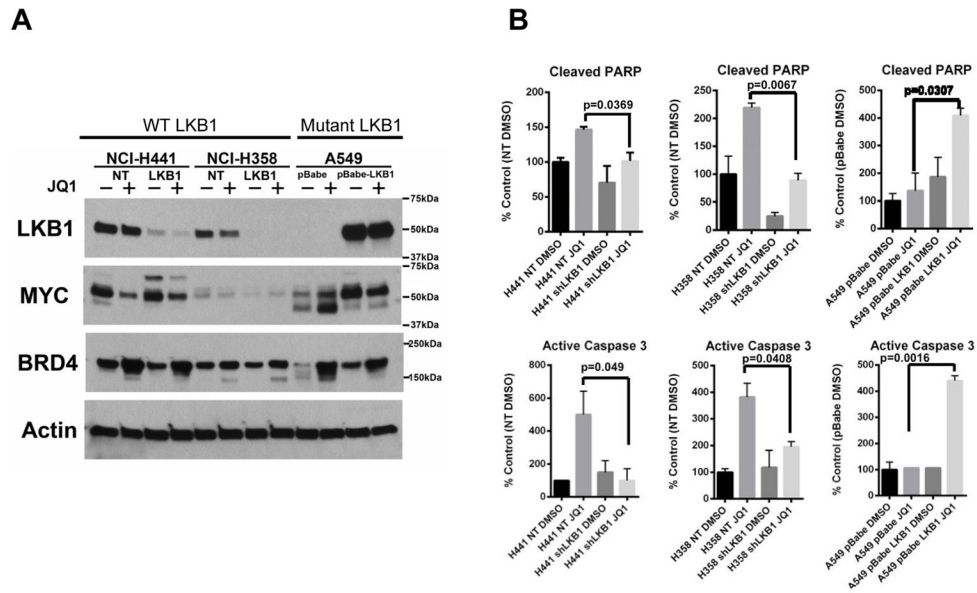
Figure 4. The loss of LKB1 renders mutant KRAS NSCLC cells resistant to JQ1
(A) Two paired LKB1 and control (non-target, NT) knockdown cells were generated in KRAS^{mut}/LKB1^{WT} NSCLC cell lines, H358 (H358LKB1 and H358NT) and H441 (H441LKB1 and H441NT). Additionally, wild-type LKB1 was ectopically expressed in KRAS^{mut}/LKB1^{mut} A549 cell line (A549 pBabe-LKB1). A549 cells were transduced with retrovirus coding for pBabe vector as a paired control (A549 pBabe). The paired cell lines were challenged with DMSO (−) or JQ1 (+) for 48 hours and lysates were subjected to Western blotting with the indicated antibodies. Note that JQ1-induced MYC depletion is modest in the mutant KRAS NSCLC cells with the loss of LKB1. (B) Exponentially growing paired NCI-H441 or NCI-H358 or A549 cells were treated with DMSO or JQ1 (500 nM) for 48 hours. Cells were harvested for Luminex-based active Caspase-3 (bottom) and cleaved PARP (top) assay for the detection of apoptosis. The induction of apoptosis markers is significantly more in cells with LKB1 than in LKB1 deficient cells. The results are from two independent experiments run with duplicate samples. Bars, S.D.
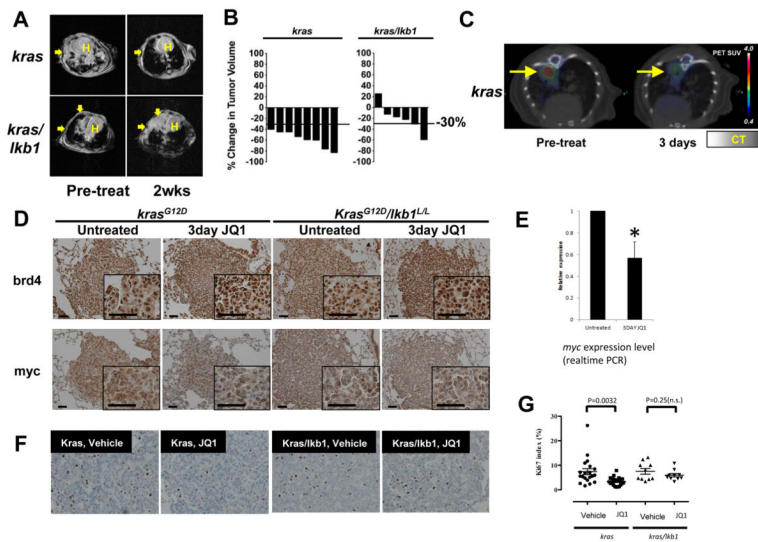
Figure 5. JQ1 promotes BRD4 accumulation and MYC depletion in a mutant *kras* murine lung cancer model

(A) Mice harboring mutant *kras* or *kras/lkb1* were subjected to MRI to establish measurable tumor burden. Next, mice were treated daily with JQ1 (50 mg/kg) by intraperitoneal injection. Two weeks post-treatment, the mice were imaged to evaluate tumor burden. Arrows indicate tumors; H indicates Heart. (B) Volumetric measurements of tumor burden in *kras* and *kras/lkb1* mice after two weeks of JQ1 treatment. *kras* mice exhibited an objective response (> 30%) to JQ1 treatment while *kras/lkb1* tumors do not respond as favorably to JQ1-treatment. (C) Representative FDG-PET/CT images of *kras* mice at baseline and 3 days post-treatment. Baseline and post-treatment PET images are depicted with identical scales. The colored FDG-PET images are superimposed with the grey-scale cross-sectional CT images. (D) Immunohistochemical (IHC) staining of lung tumors shows JQ1-treatments are more efficacious in downregulating *myc* expression in mutant *kras* mice than in mutant *kras/lkb1* mice. IHC for brd4 (Top), and myc (Bottom) of lung tumors from *kras* or *kras/lkb1* mice. Mice were treated with 3 doses of JQ1 over 3 days. The third dose was given 3 hours prior to euthanasia, and lung sections were stained with indicated antibodies. Photos shown are representative fields in each group in low and high magnification. Scale bars measure 50 μm. (E) Quantitative RT-PCR analysis of total *myc* transcript isolated from untreated and JQ1-treated mutant *kras* mice tumors shows that effects on myc mRNA expression are significantly ($p < 0.05$) with evident decreases in tumor nodules harvested from *kras* mice treated with JQ1 for 3 days. Each sample was analyzed in triplicate for quantification of both total *myc* and -actin transcripts. The endogenous mouse *myc* level from untreated mice was arbitrarily designated as 1. Data were analyzed by relative quantitation using the Ct method with normalization to -actin. Error bars, S.D. (F) Representative pictures of Ki-67 IHC staining of lung tumors from mutant *kras* and *kras/lkb1* mutant mice untreated or treated with JQ1. (G) Scoring of Ki-67 positive cells shows significant ($p = 0.0032$, Student's t-test) reduction in Ki-67 positive cells in mutant kras tumors treated with JQ1 for 3 days. Five areas of each slide were counted (n = 4 each for mutant *kras* treated and untreated; n = 2 each for *kras/lkb1* mutant treated and untreated). Error bars represent S.D.